

Controlling local temperature in water using femtosecond optical tweezer

Dipankar Mondal and Debabrata Goswami*

Indian institute of Technology Kanpur, Department of Chemistry, Kanpur 208016, Uttar Pradesh, India
*dgoswami@iitk.ac.in

Abstract: A novel method of directly observing the effect of temperature rise in water at the vicinity of optical trap center is presented. Our approach relies on changed values of corner frequency of the optical trap that, in turn, is realized from its power spectra. Our two color experiment is a unique combination of a non-heating femtosecond trapping laser at 780 nm, coupled to a femtosecond infrared heating laser at 1560 nm, which precisely controls temperature at focal volume of the trap center using low powers (100-800 μ W) at high repetition rate. The geometric ray optics model quantitatively supports our experimental data.

©2015 Optical Society of America

OCIS codes: (320.2250) Femtosecond phenomena; (350.4855) Optical tweezers or optical manipulation; (120.6780) Temperature; (010.7340) Water; (290.6815) Thermal emission.

References and links

1. A. Ashkin, J. M. Dziedzic, and T. Yamane, "Optical trapping and manipulation of single cells using infrared laser beams," *Nature* **330**(6150), 769–771 (1987).
2. S. M. Block, D. F. Blair, and H. C. Berg, "Compliance of bacterial flagella measured with optical tweezers," *Nature* **338**(6215), 514–518 (1989).
3. A. Ashkin and J. M. Dziedzic, "Internal cell manipulation using infrared laser traps," *Proc. Natl. Acad. Sci. U.S.A.* **86**(20), 7914–7918 (1989).
4. I. Bhattacharyya, P. Kumar, and D. Goswami, "Effect of isotope substitution in binary liquids with Thermal-Lens spectroscopy," *Chem. Phys. Lett.* **598**(24), 35–38 (2014).
5. P. Kumar, S. Dinda, A. Chakraborty, and D. Goswami, "Unusual behavior of thermal lens in alcohols," *Phys. Chem. Chem. Phys.* **16**(24), 12291–12298 (2014).
6. G. Herzberg, *Infrared and Raman Spectra* (D. Van Nostrand: Princeton, 1945).
7. K. König, H. Liang, M. W. Berns, and B. J. Tromberg, "Cell damage in near-infrared multimode optical traps as a result of multiphoton absorption," *Opt. Lett.* **21**(14), 1090–1092 (1996).
8. A. Ansari, C. M. Jones, E. R. Henry, J. Hofrichter, and W. A. Eaton, "The role of solvent viscosity in the dynamics of protein conformational changes," *Science* **256**(5065), 1796–1798 (1992).
9. B. Heinrich, "Why have some animals evolved to regulate a high body temperature?" *Am. Nat.* **111**(980), 623–640 (1977).
10. M. L. Begasse, M. Leaver, F. Vazquez, S. W. Grill, and A. A. Hyman, "Temperature dependence of cell division timing accounts for a shift in the thermal limits of *C. elegans* and *C. briggsae*," *Cell Reports* **10**(5), 647–653 (2015).
11. K. Svoboda and S. M. Block, "Biological applications of optical forces," *Annu. Rev. Biophys. Biomol. Struct.* **23**(1), 247–285 (1994).
12. Q. Xing, F. Mao, L. Chai, and Q. Wang, "Numerical modeling and theoretical analysis of femtosecond laser tweezers," *Opt. Laser Technol.* **36**(8), 635–639 (2004).
13. B. Agate, C. Brown, W. Sibbett, and K. Dholakia, "Femtosecond optical tweezers for in-situ control of two-photon fluorescence," *Opt. Express* **12**(13), 3011–3017 (2004).
14. A. K. De, D. Roy, A. Dutta, and D. Goswami, "Stable optical trapping of latex nanoparticles with ultrashort pulsed illumination," *Appl. Opt.* **48**(31), G33–G37 (2009).
15. A. Ashkin, "Acceleration and Trapping of Particles by Radiation Pressure," *Phys. Rev. Lett.* **24**(4), 156–159 (1970).
16. A. Ashkin, J. M. Dziedzic, J. E. Bjorkholm, and S. Chu, "Observation of a single-beam gradient force optical trap for dielectric particles," *Opt. Lett.* **11**(5), 288–290 (1986).
17. D. Mondal and D. Goswami, "Controlling the effect on solvent by resonant excitation in femtosecond optical tweezer," in *Proceedings Optics in the Life Sciences*, OSA Technical Digest (online) (Optical Society of America, 2015), paper OtT4E.3.
18. K. Berg-Sørensen and H. Flyvbjerg, "Power spectrum analysis for optical tweezers," *Rev. Sci. Instrum.* **75**(3), 594–612 (2004).

19. Y. Liu, G. J. Sonek, M. W. Berns, and B. J. Tromberg, "Physiological monitoring of optically trapped cells: assessing the effects of confinement by 1064-nm laser tweezers using microfluorometry," *Biophys. J.* **71**(4), 2158–2167 (1996).
20. K. Kwac and M. Cho, "Two-color pump-probe spectroscopies of two- and three-level systems: 2-dimensional line shapes and solvation dynamics," *J. Phys. Chem. A* **107**(31), 5903–5912 (2003).
21. G. E. Uhlenbeck and L. S. Ornstein, "On the theory of Brownian motion," *Phys. Rev.* **36**(5), 823–841 (1930).
22. M. C. Wang and G. E. Uhlenbeck, "On the theory of Brownian motion II," *Rev. Mod. Phys.* **17**(2–3), 323–342 (1945).
23. X. E. Lin, "Laser pulse heating," in *Proceedings of the 1999 Particle Accelerator Conference* (IEEE, 1999), pp. 1429–1431.
24. http://www.olympus-ims.com/en/microscope/terms/luminous_flux/.
25. T. Al-Shemmeri, *Engineering Fluid Mechanics* (Ventus Publishing ApS, 2012).
26. A. Schönle and S. W. Hell, "Heating by absorption in the focus of an objective lens," *Opt. Lett.* **23**(5), 325–327 (1998).
27. I.-M. Tolić-Nørrellykke, K. Berg-Sørensen, and H. Flyvbjerg, "MatLab program for precision calibration of optical tweezers," *Comput. Phys. Commun.* **159**(3), 225–240 (2004).
28. H. Mao, J. R. Arias-Gonzalez, S. B. Smith, I. Tinoco, Jr., and C. Bustamante, "Temperature control methods in a laser tweezers system," *Biophys. J.* **89**(2), 1308–1316 (2005).
29. M. Tassieri, F. Del Giudice, E. J. Robertson, N. Jain, B. Fries, R. Wilson, A. Glidle, F. Greco, P. A. Netti, P. L. Maffettone, T. Bicanic, and J. M. Cooper, "Microrheology with Optical Tweezers: Measuring the relative viscosity of solutions 'at a glance'," *Sci. Rep.* **5**, 8831 (2015).
30. *CRC Handbook of Chemistry and Physics*. 85th ed. (CRC Press, Boca Raton, FL 1991–1992).
31. Y. Liu, D. K. Cheng, G. J. Sonek, M. W. Berns, C. F. Chapman, and B. J. Tromberg, "Evidence for localized cell heating induced by infrared optical tweezers," *Biophys. J.* **68**(5), 2137–2144 (1995).
32. R. R. Agayan, F. Gittes, R. Kopelman, and C. F. Schmidt, "Optical trapping near resonance absorption," *Appl. Opt.* **41**(12), 2318–2327 (2002).
33. E. J. G. Peterman, F. Gittes, and C. F. Schmidt, "Laser-induced heating in optical traps," *Biophys. J.* **84**(2), 1308–1316 (2003).

1. Introduction

Laser trapping of cells, viruses, bacteria, etc. using forces of coherent radiation pressure at benign infrared (IR) wavelength of 1064 nm [1–3] have increased the range of precise bio-manipulation appliances. While the same advantages remain for benign wavelength operation at 780 nm as trapping laser, this is not true for IR laser trapping at 1560 nm, which has an increased water absorption [4, 5]. The strong vibrational combination band of hydroxyl group (OH) at 1560 nm [6] along with the non-radiative relaxation of water leads to a substantial temperature rise. Such temperature rise from 1560 nm laser may highly impact bio systems, since water is their main ingredient [7, 8]. Typically, each biological system works actively only within a certain temperature range [9]. However, there is continued interest in finding new ways to probe their behavior under different temperature gradients especially in regard to cell apoptosis and cell division [10]. Optical tweezers can, in fact, be a very effective tool to probe such behavior of bio systems [11]. We present here a novel approach of using optical tweezers in solvents having OH bond in conjunction with an IR laser at 1560 nm, utilizing the fundamental approach of applying small perturbation on the system under study. One method of providing the smallest possible perturbation is to have the minimal impact through smallest possible interaction time. In recent years, femtosecond optical tweezers [12–14] have attracted more attention over conventional continuous wave (CW) laser tweezers [15, 16]. Due to their ultra-high peak powers, femtosecond tweezers use very little average power to generate the requisite gradient force to overcome the scattering force to trap and manipulate micron to nano-sized particles. The low average power also has minimal effect on the solvent medium, though this is only true for very low absorbing media at a specific trapping wavelength. Thus, in terms of absorption wavelength selection and solvent selection are mutually dependent.

The low average power of femtosecond high repetition rate 1560 nm laser in presence of 780 nm femtosecond laser trap is able to increase temperature and decrease viscosity significantly [17]. Effect of local heating is directly observed in the corner frequency (f_c) of the optical trap deduced from its power spectrum [18] though there is no effect on its trap stiffness. Since pulse laser heating [19] is much more effective than the traditional CW laser, femtosecond pulse for local heating should increase its sensitivity as well. Femtosecond high

repetition rate IR laser with microwatt power is sufficient to change the trapping volume temperature significantly due to its high peak power. Our theoretical model also supports our experimental data. However, since this model is only based on conduction, a small amount of deviation begins to appear between our experimental and theoretical data at higher temperatures [5]. Our two color pump probe [20] experimental setup with 1560 nm acting as a pump will create perturbation at trapped volume, which directly affects the 780 nm probe laser trapping of fluorescence coated polystyrene bead. The environmental change can be easily sensed by the trapped bead, which is reflected in its Brownian motion [21, 22].

2. Experimental section

In our optical tweezers setup (Fig. 1), the laser source is an Er-doped fiber laser (Femtolite C-20-SP, IMRA Inc. USA), which generates femtosecond laser pulses centered at fundamental 1560 nm wavelength and its second harmonic 780 nm with pulse-widths 300 fs and 100 fs respectively. The two laser pulse outputs are collinear at a repetition rate of 50 MHz. To achieve tight focusing, an oil immersion objective (UPlanSApo, 100X, 1.4 NA, OLYMPUS Inc. Japan) was used and the forward scattered light was collected with another oil immersion objective (60x, PlanAapo N, 1.42 NA, OLYMPUS Inc. Japan) and focused onto a quadrant photodiode (QPD) (2901, Newport Co. USA). The QPD output was connected to a digital oscilloscope (Waverunner 64Xi, LeCroy USA) interfaced with a personal computer through a GPIB card (National Instruments, USA). Data was acquired using our LabVIEW program.

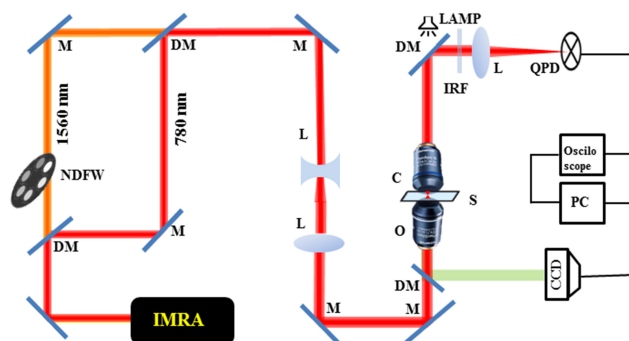


Fig. 1. Schematic diagram of our experimental femtosecond optical tweezers setup. DM: Dichroic mirror; NDFW: Neutral Density Filter Wheels; M: Mirror; L: Lens; O: Objective lens; S: Sample chamber; C: Condenser lens; IRF: Infrared filter; QPD: Quadrant photodiode; CCD: Camera (Charge coupled device).

We trapped 1.0 μm mean diameter (T8883, Life technology, USA) fluorophore coated polystyrene microsphere suspended in phosphate buffer saline solution. The video of the trapping event was monitored using CCD camera (350 K pixel, e-Marks Inc. USA). The trapping laser power was measured with a power meter (FieldMate, Coherent USA) as well as a silicon amplified photodiode (PDA100A-EC, Thorlabs USA) and 1560 nm power was measured with a calibrated biased InGaAs detector (DET10C/M, Thorlabs USA). The absorption spectrum was collected by the absorption spectrometer (Lambda 900, PerkinElmer USA). The focal point was measured using linear motorized stage (UE1724SR driven by ESP300, Newport Co. USA) interfaced with a personal computer through the GPIB card.

3. Results and discussion

3.1 Theoretical model

We calculate spot sizes for the two color focused beam generated by a single focusing objective lens that does not focus to a single point, using simple ray optics geometry (Fig. 2). Typically, the simultaneous flux calculation for two colors is complicated due to the spatial separation between two focal points as the intensity of two beams depends on their individual focal spot sizes. However, using our ray optics model we have calculated the temperature rise

at trapped volume, which quantitatively supports the experimental data. We calculate the difference between two color focal points by placing a thin cover slip sample chamber containing 10^{-4} M Rhodamine-6G in water. The maximum two photon fluorescence (TPF) is observed at the exact focal point of 780 nm laser on CCD, while at a position $1.6 \mu\text{m}$ further,

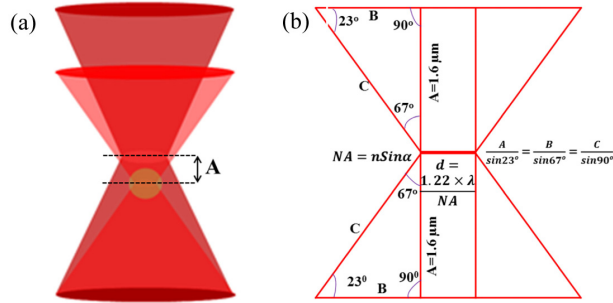


Fig. 2. (a) The focus of two colors by a single objective lens when one of higher energy color trapped the fluorophore coated polystyrene bead. (b) The geometry for calculating effective radius at a distance from focus.

the minimum transmittance signal occurs on InGaAs 1560 nm detector, which is the focal point of 1560 nm. We measured the separation between the focal points by moving a linear motorized stage (of minimum resolution 0.00001 mm). We evaluate the maximum temperature rise with respect to the room temperature (T_0) for a Gaussian pulse using [23]:

$$T_{\max} - T_0 = 0.783 \frac{F}{\tau_p} \frac{2\sqrt{\tau_p}}{\sqrt{\pi K \rho C}} \quad (1)$$

where, F is the fluence absorbed by water used in the sample chamber, τ_p is the laser pulse-width at 1560 nm, K is thermal conductivity, C is heat capacity and ρ stands for density of water. The 1560 nm is focused by 100X objective perpendicularly onto the cover slip sample chamber. The total fluence absorbed by water is $\mathcal{A} \cdot (1 - |r_f|^2) \cdot F_0$, where F_0 is laser fluence before the sample chamber and r_f is the reflection coefficient that is calculated from the refractive index, n , using relation: $r_f = (n-1)/(n+1)$. \mathcal{A} is the water absorbance in thin sample chamber.

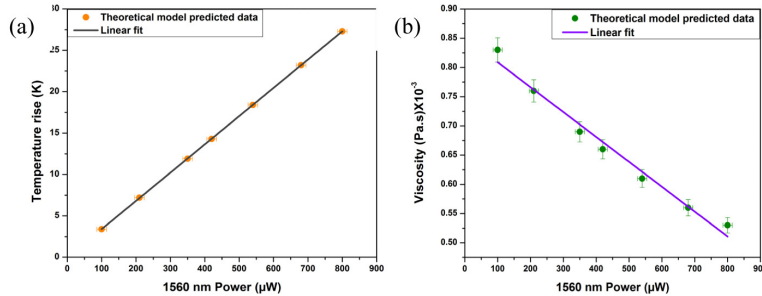


Fig. 3. (a) Our theoretical model predicted plot: temperature versus 1560 nm power (orange circle) and its linear fit (solid line). (b) Our theoretical model predicted plot: viscosity versus 1560 nm power (green circle) and its linear fit (solid line).

The half angle of the objective does not change since focal length of the 100X objective is higher (nearly 100 times) than the separation between the two focal points of two colors (Fig. 2). We can thus use the geometric model [24] to calculate effective beam waist spot size of 1560 nm laser at focus as 1360 nm and that of 780 nm laser at focus as 680 nm. These

effective beam radii can be used to calculate the pump laser (1560 nm) fluence at the 780 nm beam focus, where the polystyrene bead is trapped, with the help of the following equation:

$$F_0 = \frac{\text{PulseEnergy}}{\pi \left[\left\{ \left(\frac{\sin 67^\circ}{\sin 23^\circ} \times 1.6 \right) + .68 \right\} \times 10^{-6} \right]^2} \quad (2)$$

The viscosity change as a result of this heating can be calculated using the equation [25]:

$$T = 140 + 247.8 \times \left\{ \log \left(\frac{\eta(T)}{2.414 \times 10^{-5}} \right) \right\}^{-1} \quad (3)$$

We find that the calculated viscosity decreases linearly with increase in power of 1560 nm laser due to the inverse relationship between them in a small interval change (Fig. 3).

3.2 Experimental observation

We used a pulsed 780 nm laser of 7 mW average power to trap fluorophore coated polystyrene microspheres. The trapping laser has a nominal heating effect [26] on the trapped bead because of the very low absorption coefficient of water at 780 nm. At 1560 nm, however, water has a high absorption coefficient due to the strong vibrational combination band. As the absorption coefficient is completely dependent on path length or sample thickness, our experimentally measured absorbance in the very thin cover slip sample chamber is only 0.108. However, this absorbance is sufficient to be utilized for precise control of the temperature of the micron size trapping volume. The low power illumination of femtosecond high repetition rate 1560 nm can change the focal volume temperature and viscosity effortlessly, which should be directly reflected by the characteristics of the trapped fluorophore coated polystyrene microsphere.

We analyzed the forward scattered data of trapped bead collected with QPD at 20 kHz sampling rate for 2.5 seconds duration. The acquired data of channel X and Y is de-correlated by removing the cross-talk [18, 27] between them. The processed data was then fitted with the following Lorentzian function:

$$P_x(f) = \frac{A}{(f_c^2 + f^2)} \quad (4)$$

The fitting parameter A gives us information about the diffusion coefficient. The corner frequencies are derived from the fitted power spectra (Fig. 4). Additionally, the inverse of corner frequency linearly decreases with an increase in the 1560 nm power (Fig. 5(a)) though the linear dependence is not expected to continue beyond certain temperature range (Fig. 5(b)).

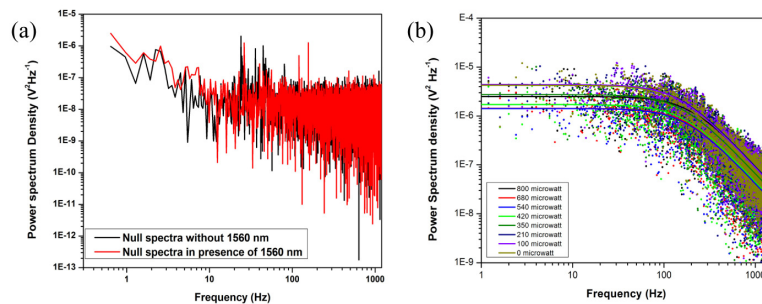


Fig. 4. (a) Experimentally measured power null spectra and (b) power spectrum (Scatter points) and respective Lorentzian fitted data (Solid line) for 1µm fluorophore coated polystyrene bead.

Within our experimental range of temperatures, even viscosity is linearly dependent on inverse of corner frequency [28]. This may be due to change in trap stiffness or due to a change in viscosity of the solvent, which is directly dependent on solvent temperature as a result of thermal emission due to non-radiative relaxation process. As our trapping power is fixed and pump power (1560 nm) is very small, we can narrow this down to the viscosity change due to local heating. Focal point temperature is directly proportional to the pump power. Viscosity linearly decreases with temperature for small temperature interval as calculated from our theoretical model used (Fig. 3). Under this condition, we calculate the viscosity at different powers relative to 0.89×10^{-3} Pa.s (corresponding to $f_c = 131$ Hz at 298 K) [30], which is the water viscosity at 298 K when 1560 nm laser is absent. Within the range of our experimental conditions, we approximate that $f_c \propto \eta$ as a constant [28, 29]. We find that the maximum viscosity decrease ($\Delta\eta$) is 0.30×10^{-3} Pa.s, which is observed at 800 μ W power of 1560 nm. This observed value is within $\sim 5\%$ error bar.

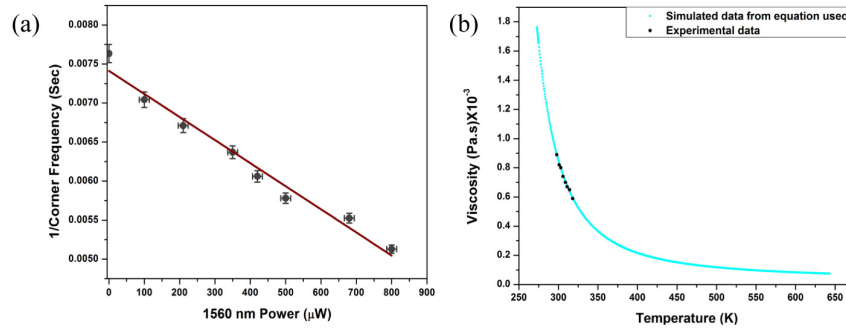


Fig. 5. (a) Plot of Inverse corner frequency versus power of 1560 nm femtosecond laser with linear fitting (Brown line). (b) Plot of viscosity versus temperature for experimental (black circle) and simulated data (Cyan line).

Using the corresponding observed viscosity, we calculate temperature at different powers of 1560 nm from Eq. (2). We also calculated trap stiffness ($\kappa = 2\pi\gamma f_c$) using viscous drag coefficient ($\gamma = 6\pi\eta r$) of polystyrene bead of radius r , which was found to be almost constant though temperature was increasing. Our calculated trap stiffness (κ_{ps}) from power spectrum is 0.0068 ± 0.0001 pN/nm. Table 1 summarizes all calculated data and measured parameters.

Table 1. Comparison between our theoretical and experimental data

1560 nm Power (μ W)	Corner Frequency (Hz)	Fluence (J/m^2)	Theoretical data		Experimental data	
			$T_{max} - T_0$ (K)	Viscosity (Pa.s) $\times 10^{-3}$	Temperature rise (K)	Viscosity (Pa.s) $\times 10^{-3}$
100	142	0.0322	3.4	0.83	3	0.82
210	149	0.0675	7.2	0.76	5	0.80
350	157	0.1126	11.9	0.69	8	0.74
420	165	0.1351	14.3	0.66	11	0.70
540	173	0.1737	18.4	0.61	13	0.67
680	181	0.2187	23.2	0.56	16	0.64
800	195	0.2573	27.3	0.53	20	0.59

As far as we know, this is the first report on resonantly excited optical trap temperature by femtosecond Megahertz repetition rate pulses, which is much more efficient for producing heat as compared to the CW laser induced heating [31–33] at the trapping focal volume. This efficient heating effect is evident from Table 1.

4. Conclusion

Non-radiative relaxation of water with resonant excitation sharply changes water temperature around the optical trap center. Pulsed high repetition rate 1560 nm laser having high peak power and very low average power can be very useful for alteration of temperature for highly absorbing solvents, which relax through thermal emission. In the vicinity of trapped polystyrene bead, viscosity decreases linearly with increase of 1560 nm laser power, whereas the temperature increases linearly. Our experimental setup would be very useful to generate precise temperature at a desired location. Our proposed geometrical optics model helps to understand the necessity of pulsed IR laser for creating the precise hot spot.

Acknowledgments

We thank the Wellcome Trust Senior Research Fellowship UK and DST, India for funding our research. We thank the funding support of ISRO Science Technology Cell and MHRD, Govt. of India. DM thanks UGC, India for graduate fellowship and Debjit Roy for useful discussion. We also thank Ms. S. Goswami for language edits in the article.